JCI insight

RESEARCH ARTICLE

Aldehyde dehydrogenase inhibition blocks mucosal fibrosis in human and mouse ocular scarring

Sarah D. Ahadome,[1] David J. Abraham,[2] Suryanarayana Rayapureddi,[3] Valerie P. Saw,[4] Daniel R. Saban,[5] Virginia L. Calder,[1] Jill T. Norman,[3] Markella Ponticos,[2] Julie T. Daniels,[1] and John K. Dart[4]

[1]Ocular Biology and Therapeutics, UCL Institute of Ophthalmology, London, United Kingdom. [2]Centre for Rheumatology and Connective Tissue Diseases, University College London, Royal Free Campus, London, United Kingdom. [3]Centre for Nephrology, University College London, Royal Free Campus, London, United Kingdom. [4]NIH Research (NIHR) Biomedical Research Centre at Moorfields Eye Hospital NHS Foundation Trust and the UCL Institute of Ophthalmology, London, United Kingdom. [5]Duke University School of Medicine, Departments of Ophthalmology and Immunology, Durham, North Carolina, USA.

Mucous membrane pemphigoid (MMP) is a systemic mucosal scarring disease, commonly causing blindness, for which there is no antifibrotic therapy. Aldehyde dehydrogenase family 1 (ALDH1) is upregulated in both ocular MMP (OMMP) conjunctiva and cultured fibroblasts. Application of the ALDH metabolite, retinoic acid (RA), to normal human conjunctival fibroblasts in vitro induced a diseased phenotype. Conversely, application of ALDH inhibitors, including disulfiram, to OMMP fibroblasts in vitro restored their functionality to that of normal controls. ALDH1 is also upregulated in the mucosa of the mouse model of scarring allergic eye disease (AED), used here as a surrogate for OMMP, in which topical application of disulfiram decreased fibrosis in vivo. These data suggest that progressive scarring in OMMP results from ALDH/RA fibroblast autoregulation, that the ALDH1 subfamily has a central role in immune-mediated ocular mucosal scarring, and that ALDH inhibition with disulfiram is a potential and readily translatable antifibrotic therapy.

Introduction

Fibrosis is the result of the complex cascade of cellular and molecular responses that follow tissue injury, progressing beyond tissue repair, to a process detrimental to organ function and culminating in organ failure. This is common in many chronic diseases, with scleroderma, cirrhosis, pulmonary, and renal fibrosis being among the most widely studied scarring disorders (1). Mucosal scarring has been less widely studied and is a consequence of mucous membrane pemphigoid (MMP), a prototypical multisystem autoimmune scarring disease (2). As in many other fibrotic disorders, this scarring is associated with inflammation (1). Although the role of autoantibody-mediated inflammation and blistering at the level of the epithelial basement membrane in MMP is reasonably well understood, the pathogenesis of scarring is not (3). One or more mucosal sites may be involved in MMP, with frequent and severe functional consequences (2). Ocular involvement in MMP (OMMP) occurs in 70% of cases, blinding 20% of patients (4–6). There is no effective antifibrotic therapy. This series of studies of conjunctival scarring in OMMP aimed to identify therapies for conjunctival fibrosis and, potentially, for fibrosis at other mucosal sites.

OMMP was chosen for these studies, as the conjunctiva is accessible to biopsy for in vitro investigations and because it is the most common cause of cicatrizing (scarring) conjunctivitis in the UK (7) — and probably in all developed countries where trachoma has been eliminated. Additional causes of cicatrizing conjunctivitis include atopic keratoconjunctivitis (AKC), Stevens-Johnson syndrome (SJS), and trachoma, among others (7, 8). The morbidity of OMMP is due to the chronic discomfort and loss of vision (5) caused by both inflammation and scarring. Topical therapy is ineffective for OMMP (9–11), resulting in systemic immunosuppressive therapy being the standard of care (12). However, immunosuppression, with its accompanying side effects and failures, has a limited effect on the pro-

Authorship note: JTD and JKD contributed to the manuscript equally.

Conflict of interest: SDA and DJA are inventors for Patent PCT/GB2015/051292 held by UCL Business PLC.

Submitted: February 9, 2016
Accepted: July 7, 2016
Published: August 4, 2016

Reference information:
JCI Insight. 2016;1(12):e87001.
doi:10.1172/jci.insight.87001.

gression of scarring (6, 13) despite clinical control of inflammation (5, 6). Development of effective and well-tolerated antifibrotic therapy has been a long-term goal in this group of diseases (5, 8, 14).

The pathogenesis of scarring in OMMP results from chronic inflammation involving T cells, macrophages, DCs (15). Levels of both proinflammatory cytokines TNF (16), IFNγ (17), IL-5 (18), IL-13 (19), and IL-17 (20) and the profibrotic cytokines TGFβ (21) and IL-4 (18, 22) are elevated in diseased tissue. However, the mechanisms that relate this inflammatory milieu to the production of the extracellular matrix (ECM) by fibroblasts, which results in scarring, have not been demonstrated (3, 23, 24). We have previously shown that OMMP fibroblasts maintain a profibrotic phenotype in vitro and that progressive fibrosis may result from inflammation coupled with the activity of such persistently profibrotic fibroblasts (25). For the current series of studies, we hypothesized that we might use gene expression to identify potential therapeutic targets, common to both OMMP whole conjunctiva and in vitro fibroblast cultures, to identify antifibrotic therapeutic targets in vitro. Furthermore, these targets could then be used to predict the effect of potential therapeutic interventions in humans by extrapolation from their effect in vitro on OMMP fibroblast functional assays and also in vivo in a mouse model used as a surrogate for OMMP.

Here, we present evidence that aldehyde dehydrogenase family 1 (ALDH1) is upregulated in OMMP whole conjunctiva, in OMMP fibroblasts in vitro, and in the conjunctiva of an established mouse model of severe allergic eye disease (AED) (26, 27), which also provides a surrogate for immune-mediated conjunctival scarring, given our hypothesis that the scarring is the result of the severity of the inflammatory stimulus rather than the autoimmune pathogenesis in OMMP. ALDH inhibition is effective both in preventing scarring in vivo in the mouse model and also in restoring normal functionality to in vitro OMMP fibroblasts. These studies identify ALDH/RA autoregulation in OMMP fibroblasts as a potential mechanism underlying progressive conjunctival scarring in this disease. A companion paper by Saban and colleagues using the same mouse model of AED, first described by their group in 2012 (26, 27, 28), demonstrates that conjunctival scarring is initiated by the key role of DCs through paracrine production of ALDH/RA effecting conjunctival fibroblasts. ALDH inhibition may be expected to slow progression of fibrosis in both OMMP and also potentially in other causes of cicatrizing conjunctivitis.

Results

OMMP and control patients. Twenty-two OMMP patients, 11 from inflamed and 11 from uninflamed eyes, donated biopsies for these studies. Tissue from both inflamed and uninflamed eyes was used to establish whether the degree of inflammation might be associated with functional differences in explanted in vitro fibroblast assays. However, Table 1 shows that both the inflamed and uninflamed eyes were of equivalent severity in terms of the severity of scarring, and it shows that the uninflamed cases had also had the disease for longer. The diagnosis of MMP was confirmed by direct immunofluorescence (DIF) microscopy for all cases. These were matched with 17 controls for age and sex. The clinical characteristics are summarized in Table 1, and controls are summarized in Table 2. Figure 1 illustrates the clinical spectrum of OMMP.

Endogenous ALDH1A3 levels in the conjunctiva of OMMP patients are elevated. Gene expression microarray of normal and OMMP conjunctiva was carried out to identify fibrosis-associated molecules that might be therapeutic targets. Because we had hypothesized that there might be differences in the fibrotic process between inflamed and uninflamed conjunctiva due to the potential effects of the inflammatory milieu, the whole conjunctival biopsies were from patients with clinical inflammation (pemphigoid inflamed [PemI]), patients without clinical inflammation (pemphigoid uninflamed [PemU]), and controls (C). Furthermore, since we had also hypothesized that in vitro fibroblast functional assays might be used to predict the effect of therapeutic interventions in vivo, we carried out these gene expression microarray analyses both on whole conjunctiva and on primary conjunctival fibroblasts (F) cultured from additional conjunctival biopsies from inflamed OMMP, and uninflamed OMMP, and control eyes (F-PemI, F-PemU, and F-C, respectively). *SEC13* (Supplemental Figure 1A), *CD24* (Supplemental Figure 1B), and *ALDH1A3* (Figure 2, A and B) were the only genes with associated profibrotic functions that were upregulated in both conjunctival tissue and in cultured fibroblasts. Of these genes, only *ALDH1A3* mRNA expression was shown by quantitative PCR (qPCR) to be consistently elevated in cultured OMMP fibroblasts (Figure 2C). IHC of tissue sections confirmed increased expression of ALDH1A3 in OMMP conjunctiva (Figure 2D). Flow cytometry confirmed both increased expression of ALDH1 and increased enzymatic activity in cultured diseased fibroblasts (Figure 2E). Furthermore, the addition of the ALDH1 inhibitor diethylaminobenzaldehyde (DEAB) to F-PemI and F-PemU fibroblasts decreased ALDH1 enzymatic activity (Figure 2F). Addition of all-*trans*-RA (ATRA), a metabolic

Table 1. Clinical characteristics of ocular mucous membrane pemphigoid (OMMP) patients.

ID[A]	Age	Sex	Race	Eye	Disease years[B]	Tauber[C] Right eye	Tauber Left eye	Treatment at time of biopsy[D]	Previous treatments
INFLAMED MMP PATIENTS (n = 11) (Inflammation score ≥ 5 on a scale from 1–4 for each bulbar quadrant, with a maximum score of 16)									
SP4	81	M	W[E]	RE	4	IId IIIc(5)	IId IIIa(2)	Topical steroid	Dapsone, mycophenolate, entropion surgery right eye
SP5	73	F	W	RE	16	IIc IIIa (1)	IIc	None	Azathioprine
SP6	65	M	W	RE	3.5	IIb IIIb(4)	IId IIId(3)	Sulfasalazine	Mycophenolate, cyclophosphamide, rituximab
SP8	82	F	W	RE	4	IId IIIa(1)	Not biopsied	Topical glaucoma	Mycophenolate
SP10	71	F	W	LE	1	I	IId IIIc(4)	None	Prednisolone
SP12	57	F	B[F]	Both	5	Enucleated	IIb	None	None
SP15	76	F	W	Both	2	IId IIId(6)	IId IIId(6)	Topical steroid	Dapsone
SP21	54	M	W	RE	9	IIc IIa(2)	ND[D]	Mycophenolate, dapsone, prednisolone	Mycophenolate
SP22	87	M	W	Both	1	IId IIIb(3)	IId IIIb(2)	Topical glaucoma	Doxycycline
SP23	73	F	W	LE	6	ND	IIb IIIa(1)	None	None
RI23	37	F	W	RE	1	IIc IIIa (2)	IIc IIIb (2)	None	None
UNINFLAMED MMP PATIENTS (n = 11) (Inflammation score 4 or less on a scale from 1-4 for each bulbar quadrant with a maximum score of 16)									
SU2	64	F	W	Both	1.25	IIa IIIb	IIa IIIb	None	Sulphamethoxypyridazine, Prednisolone
SU6	51	M	A[G]	Both	0.75	IIe IIIc(4)	IId IIId(2)	Cyclophosphamide, topical steroid	None
SU8	58	F	W	RE	21	IIc IIIa	IIc IIIa	Lubricants	Mycophenolate
SU10	62	M	W	RE	3	IIb IIIc(4)	IIb IIIc(3)	Dapsone	None
SU15	67	M	W	LE	12	ND	IId IIIb(3)	Dapsone, mycophenolate	Cyclophosphamide, prednisolone
SU18	73	F	W	LE	2	IIb IIIa(1)	IIa	Topical steroid	None
SU19	81	F	W	LE	25	IIb IIIa(1)	IIc IIIb(2)	Dapsone, methotrexate	None
SU22	92	M	W	RE	1	IV	I	Mycophenolate	None
RU13	70	F	W	RE	11	IIc IIIb (2)	IIc IIb (2)	Mycophenolate	Prednisolone, mycophenolate,
RU14	64	M	A	RE	8	IIa IIIa (1)	IIa IIIa (1)	Mycophenolate	Azathioprine, prednisolone
RU18	83	F	W	RE	9	IIc IIIb (2)	IIc IIIb (2)	None	Mycophenolate, sulfasalzine, dapsone

Biopsies were obtained from patients with MMP confirmed by direct immunofluorescence (DIF) microscopy, which is required for the gold standard diagnosis of MMP(47). Most patients donated biopsies from both eyes. The biopsy site was the bulbar conjunctiva in all patients. The degree of scarring in the OMMP conjunctiva was measured using the Tauber scoring system(48) in which minimal subconjunctival scarring is scored as Stage I, progressing through increasing degrees of lower conjunctival fornix reduction (Stage IIa–d) and horizontal involvement by symblepharon (Stage III a-d [n]), where [n] is the number of symblephara, to a frozen globe (Stage IV). The patients were matched for age and sex with 17 controls (median age 78, range 54-93 years, 7 Male:10 Female). [A]Subject ID, [B]years from disease onset, [C]Tauber score measures the degree of lower fornix scarring, [D]topical lubricants not included, [E]ethnic white, [F]black, [G]Asian.

product of ALDH, to F-C fibroblasts enhanced ALDH activity (Figure 2F). These data show that ALDH1 is upregulated in both OMMP whole tissue and in OMMP fibroblasts in culture.

Topical application of disulfiram decreases ocular surface inflammation of mice with AED and protects them from conjunctival fibrosis in vivo. There is currently no animal model of OMMP. An established mouse model of AED conjunctivitis (26, 27) was assessed for the presence of conjunctival fibrosis, which was found both to be present and to progress after sensitisation, mimicking the process in OMMP. This model was then used as an OMMP surrogate for the evaluation of ALDH-mediated profibrotic activity both in vitro and in vivo.

In vivo topical eye drops of ovalbumin (OVA) were applied, with or without disulfiram, to the ocular surface of previously OVA-sensitized mice over 7 days, and both inflammation and fibrosis were scored daily. In vitro mouse primary conjunctival fibroblasts were explanted and cultured to validate the role of

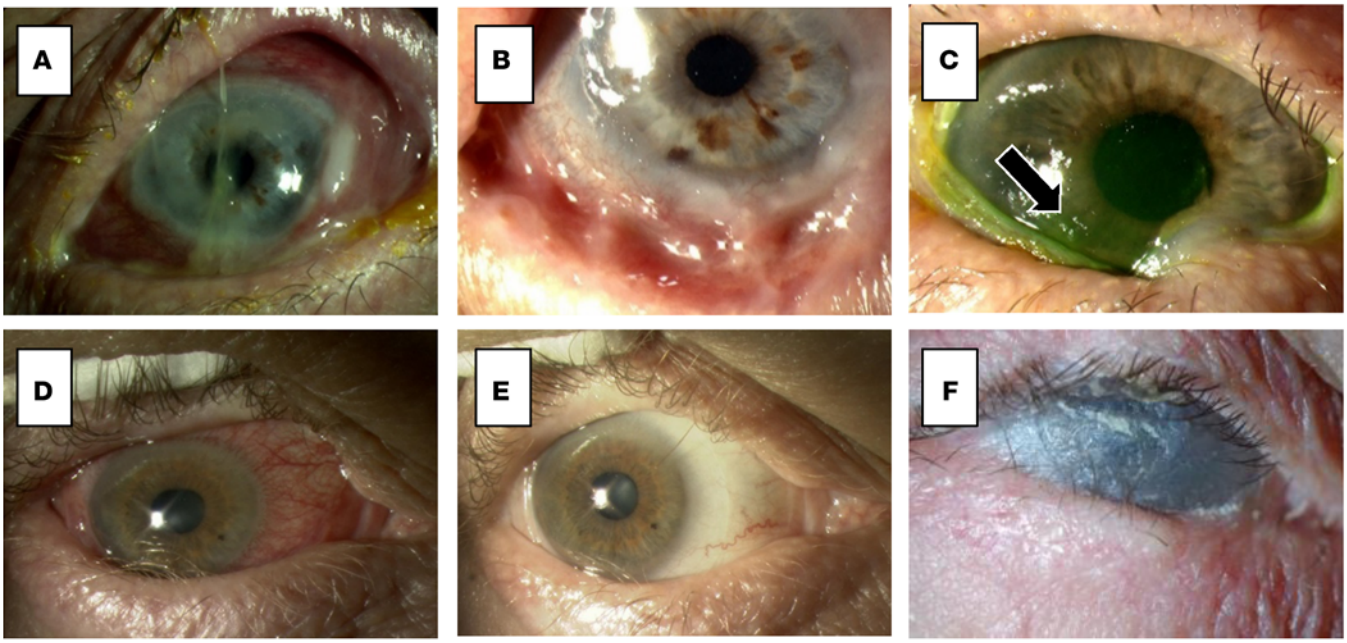

Figure 1. Ocular mucous membrane pemphigoid (OMMP): Clinical spectrum and morbidity. (**A**) Acute inflammation resulting in conjunctival scarring after 4 months. (**B**) Same eye as shown in **A** after partial control of inflammation with cyclophosphamide and prednisolone. (**C**) More advanced scarring resulting in restricted lid and eye movement and secondary corneal drying (arrow) due to reduced rewetting by the lids. (**D**) In-turning lower lid (entropion) and lash abrasion (trichiasis) in an inflamed (pemphigoid inflamed [PemI] phenotype) eye with resolution of inflammation (pemphigoid uninflamed [PemU] phenotype) in the same eye shown in **E** but 2 years after initial immunosuppressive treatment with cyclophosphamide and prednisolone, followed by dapsone for maintenance of inflammation control. (**F**) End-stage OMMP with the lids fused to the globe (frozen globe or ankyloblepharon) and extreme dryness leading to surface keratinization.

ALDH in mouse fibroblast function using some of the same in vitro assays used in our studies on human OMMP fibroblasts, which are described below.

There was increased expression of ALDH1 in the conjunctiva of mice treated with OVA (Figure 3A). Disulfiram administration decreased ocular surface inflammation (Figure 3B) and prevented conjunctival fibrosis in OVA-treated mice (Figures 3, C and D). Explanted fibroblasts from the conjunctiva of disulfiram-treated, OVA-challenged mice showed increased levels of contraction and proliferation compared with those obtained from OVA-challenged mice treated with vehicle (Figure 3E).

These data suggest that ALDH-mediated conjunctival fibrosis mechanisms exist in vivo in this mouse model of AED-mediated fibrosis. Furthermore, there is similar fibroblast functionality between conjunctival fibroblasts from OVA-treated mice and OMMP fibroblasts in vitro: explanted cultured mouse conjunctival fibroblasts display the same abnormalities, in two functional assays, as those found in in vitro human OMMP and control fibroblasts (described in the next section and in Figure 4). These data demonstrate that this AED mouse model may be used as a surrogate for the study of the mechanisms of inflammation-related conjunctival fibrosis in humans.

Primary conjunctival fibroblasts from OMMP patients maintain a fibrotic phenotype in vitro and can be used as an in vitro scarring model. F-PemI and F-PemU fibroblasts were shown to maintain increased ALDH1 activity in vitro (Figure 2, E and F). It was hypothesized that if F-PemI and F-PemU fibroblasts maintained differences from F-C fibroblasts in in vitro functional assays, then these assays might be used in an in vitro model to evaluate the role of ALDH1 on fibroblast dysregulation in vivo, both in humans and in the mouse model, and to predict the effect of potentially therapeutic interventions. The in vitro fibroblast assays chosen were collagen production and secretion, matrix contraction, proliferation, and α-smooth muscle actin (αSMA) expression, all cellular activities commonly associated with fibrotic responses.

Compared with control fibroblasts (F-C fibroblasts) both groups of OMMP fibroblasts (F-PemI and F-PemU) showed a significant increase in collagen production by ELISA (Figure 4A). Western blotting for COL1 (Figure 4B) confirmed increased matrix protein expression in F-PemI compared with F-C fibroblasts. Although there was a trend for increased COL1 expression in F-PemU compared with F-C

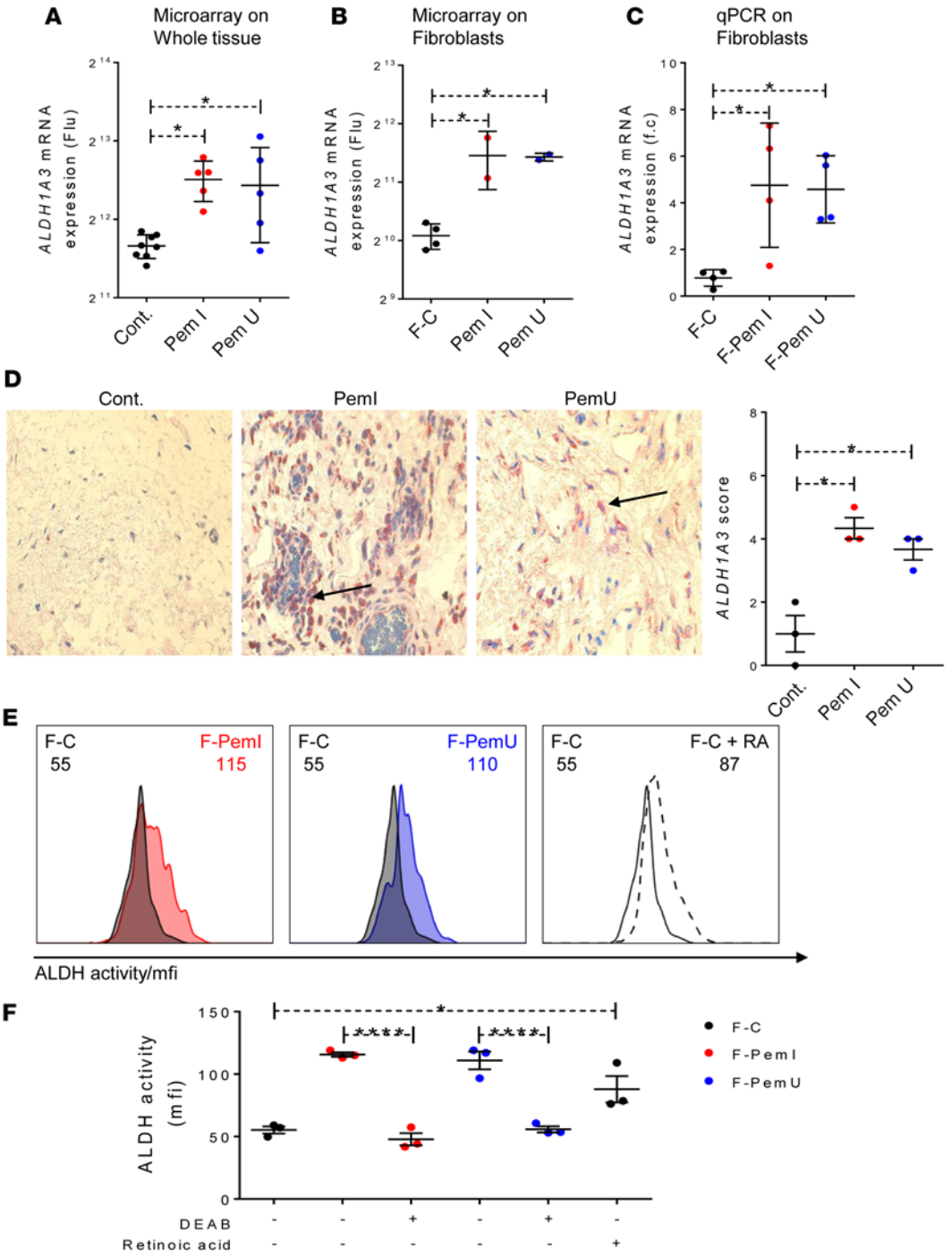

Figure 2. Aldehyde dehydrogenase (ALDH) is upregulated in the conjunctiva of OMMP patients compared with control patients. (**A**) *ALDH1A3* mRNA expression in conjunctival biopsies from control patients (Cont., *n* = 5), inflamed OMMP patients (PemI, *n* = 5), or noninflamed (after immunosuppressive treatment) OMMP patients (PemU, *n* = 5). (**B** and **C**) *ALDH1A3* mRNA expression in primary conjunctival fibroblasts obtained from Cont. (primary cultured fibroblasts from controls [F-C], *n* = 4) compared with fibroblasts from pemphigoid inflamed (F-PemI, *n* = 4) or pemphigoid uninflamed (F-PemU, *n* = 4) from the microarray and qPCR. The microarray was carried out in duplicate and the qPCR in triplicate. (**D**) Representative immunohistochemical staining for ALDH1A3 in Cont. (*n* = 3), PemI (*n* = 3), and PemU (*n* = 3). Arrows indicate positive staining for ALDH1A3. ALDH1A3-positive staining was scored on a scale of 0–5 for each tissue section from these tissue samples, with 5 being highest level of ALDH1A3-positive staining. 40× magnification. (**E**) Flow cytometry analysis of mean fluorescence intensity (MFI) of ALDEFLOUR (an ALDH1 substrate that only fluoresces once it has been metabolized by ALDH) in F-C (*n* = 3), F-PemI (*n* = 3), or F-PemU (*n* = 3) fibroblasts. (**F**) MFI of ALDH activity of F-PemI (*n* = 3) and F-PemU (*n* = 3) fibroblasts treated with diethylaminobenzaldehyde (DEAB) or F-C (*n* = 3) fibroblasts treated with retinoic acid. Error bars represent mean ±SEM. **P* < 0.05 and *****P* < 0.00005 as calculated using one-way ANOVA with Bonferronni correction

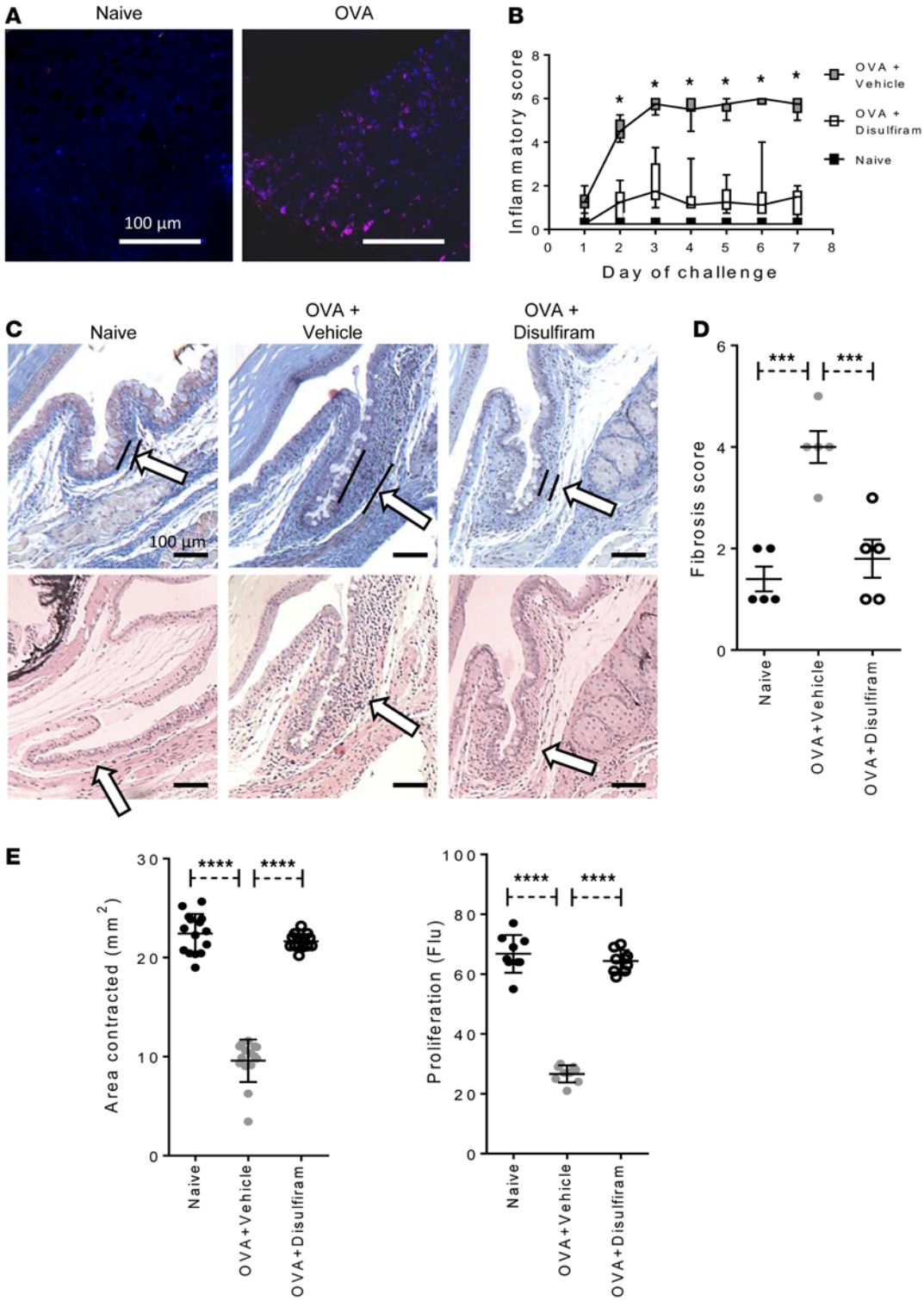

Figure 3. Topical application of disulfiram decreases ocular surface inflammation of mice with ovalbumin-induced conjunctivitis and protects them from conjunctival fibrosis in vivo. (**A**) Expression of ALDH1 in mouse conjunctiva. (**B**) Ocular surface inflammatory score in ovalbumin-treated (OVA-treated) mice (n = 5) treated daily with topical eye drops containing disulfiram or vehicle for a 7-day antigen challenge period. Naive mice (n = 5) without OVA challenge were also monitored in the same manner throughout the challenge period. (**C**) Representative histological staining for collagen (MSB, dark blue) and inflammatory infiltrate (H&E) of whole eye sections from naive mice (n = 5) and OVA-challenged mice (n = 5) treated with either disulfiram (300 μM) or vehicle. Arrows and lines indicate differences in collagen accumulation in the MSB panel and visual changes in cellular infiltrate in the H&E panel. (**D**) Quantitation of fibrosis for naive, OVA + vehicle, and OVA + disulfiram groups (n = 5). The histology images were scored on a scale of 0–5 for each tissue section from these tissue samples, with 5 being highest intensity of MSB staining. (**E**) Primary conjunctival fibroblasts (n = 5 mouse cultures) were explanted from naive mice and OVA-challenged mice treated with disulfiram or vehicle. Fibroblasts were assessed for contractility (left panel) and proliferation (right panel). Scale bars: 100 μm. Error bars represent mean ±SEM. *P < 0.05, ***P < 0.0005, ****P < 0.00005 as calculated using one-way ANOVA with Bonferroni correction.

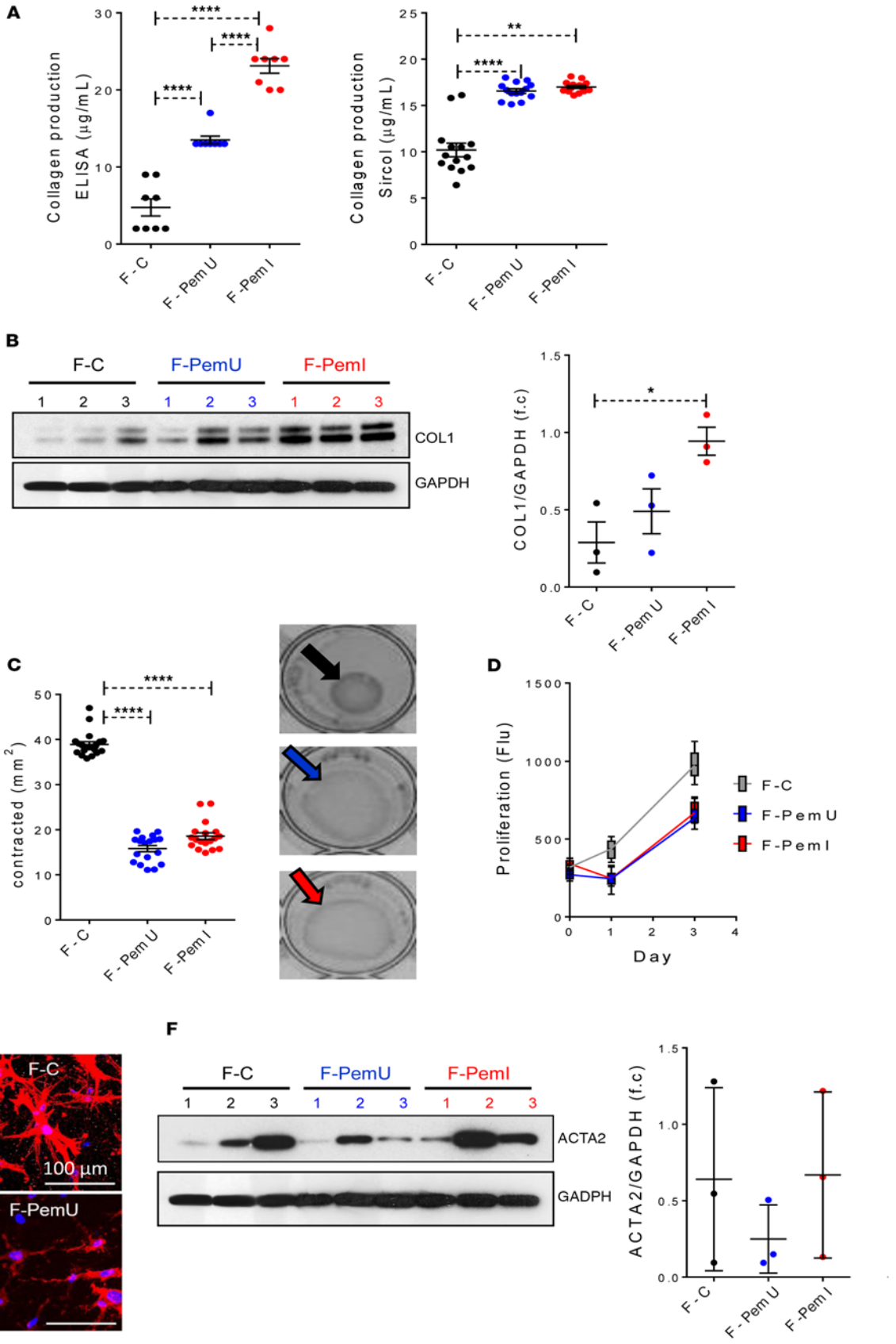
A
Collagen production ELISA (µg/mL)
Collagen production Sircol (µg/mL)
F-C
F-PemU
F-PemI
B
F-C
F-PemU
F-PemI
COL1
GAPDH
COL1/GAPDH (f.c)
C
Area contracted (mm²)
D
Proliferation (Flu)
Day
E
F-C
100 µm
F-PemU
F
ACTA2
GADPH
ACTA2/GAPDH (f.c)

Figure 4. Primary conjunctival fibroblasts from OMMP patients maintain a fibrotic phenotype in vitro. (**A**) Concentration of collagen from ELISA and Sircol assays from F-C (n = 4), F-PemI (n = 4), and F-PemU (n = 4) fibroblasts. (**B**) Basal COL1 levels were also measured by Western blotting for F-C (n = 3), F-PemU (n = 3), and F-PemI (n = 3); the densitometry shows significant differences for F-PemI compared with F-C fibroblasts. There is a trend for a difference between F-PemU and F-C, but this was not statistically significant. (**C**) Area contracted at 72 hours by F-C (n = 4), F-PemI (n = 4), or F-PemU (n = 4) fibroblasts in free-floating collagen gels. The arrows indicate the edge of the gels. (**D**) Proliferation measured by fluorescence intensity (counts per second [cps]) from F-C (n = 4), F-PemI (n = 4), or F-PemU (n = 4) fibroblasts labeled with the fluorescent CyQuant nucleotide dye. (**E**) Tethered collagen gels populated with F-C (n = 4), F-PemI (n = 4), or F-PemU (n = 4) fibroblasts were stained for αSMA (red) and nuclei stained with DAPI (blue). Each assay was carried out with 4 separate patient fibroblast cultures and at least 3 technical repeats. (**F**) αSMA levels were also measured by Western blotting and densitometry for basal F-C (n = 3), F-PemU (n = 3), and F-PemI (n = 3). Error bars represent mean ±SEM. *P < 0.05; **P < 0.005; ****P < 0.00005 as calculated using one-way ANOVA with Bonferroni correction. Scale bar: 100 μm.

fibroblasts, this did not achieve the statistical significance seen in ELISA. Figure 4, C–E, shows lower levels of contraction and proliferation and less organized αSMA compared with controls. Western blotting for αSMA showed no difference in expression between F-C, F-PemU, and F-PemI (Figure 4F), demonstrating that the organizational change shown by immunofluorescence (Figure 4E) was not associated with altered αSMA levels (see Supplemental Figure 4 for full uncut gels). There was similar functionality, and αSMA organizational change, in fibroblasts from inflamed and uninflamed OMMP conjunctiva. These data confirmed that F-PemI and F-PemU fibroblasts maintain a profibrotic phenotype in vitro and that these assays could be used to assess the potential role of profibrotic proteins, including ALDH1, in OMMP.

ALDH inhibition decreases collagen production, increases matrix contraction and proliferation, and increases αSMA expression of OMMP fibroblasts in vitro. To evaluate whether the ALDH1 family and/or other ALDH families are involved in the profibrotic phenotype, the effect of ALDH inhibition on OMMP fibroblasts was assessed. The ALDH inhibitors, DEAB and disulfiram, were used. DEAB is a competitive substrate for the ALDH1 family (29), whereas disulfiram is an irreversible inhibitor of ALDH families 1–3 (29), The inhibitory effect of disulfiram is mediated by its metabolic product diethyldithiocarbamate (DDTC, also known as ditiocarb) and its downstream metabolites (29, 30). We also used the assays described in Figure 4 to evaluate whether mimicking the effect of enhanced ALDH activity in F-C fibroblasts — by addition of the ALDH1 metabolite ATRA — would induce a profibrotic phenotype similar to that of OMMP fibroblasts. Treatment of F-PemI and F-PemU fibroblasts with DEAB and disulfiram significantly reduced collagen levels, as shown by ELISA (Figure 5A); enhanced contraction and proliferation; and altered αSMA organization (Figure 5, C–E) compared with F–C fibroblasts. In contrast, addition of RA to control fibroblasts (F-C) significantly increased collagen production, and decreased rates of contraction and proliferation and altered αSMA organization (Figure 5, A and C–E). The effect of DEAB, disulfiram, and RA was dose dependent (Supplemental Figure 2, A–C) with DEAB 1×10^{-5} M, disulfiram 1×10^{-7} M, and RA 1×10^{-2} M being the most effective dose. Western blotting was used to confirm the results demonstrated by ELISA for cell-associated collagen levels in response to treatment with disulfiram shown in Figure 5B and for F-C fibroblasts with ATRA in Supplemental Figure 3B. This confirmed the findings by ELISA for the effect of disulfiram on collagen levels in F-PemI and for ATRA on F-C. However, disulfiram had no effect on collagen levels in F-PemU. These data suggest that the raised levels of the ALDH1 subfamily, and/or ALDH1A3, in the conjunctiva of OMMP patients may directly contribute to scarring by inducing profibrotic fibroblast functions. qPCR for *COL1A2* and *COL1A3* (Supplemental Figure 3A) showed no differences in mRNA expression between F-C, F-PemU, and F-PemI both for basal levels and for fibroblasts treated with disulfiram and ATRA, showing that the effects of ALDH/RA are unlikely to be due to a translational or posttranslational effect on COL gene expression.

Overall, these data in human OMMP fibroblasts in vitro and in an in vivo mouse model provide proof of concept that disulfiram may be repurposed for the therapy of conjunctival scarring in OMMP in inflamed and possibly in the uninflamed OMMP conjunctiva.

Discussion

These studies were designed to identify and validate therapeutic targets for the treatment of conjunctival fibrosis in OMMP patients. We have shown both that ALDH1 is upregulated in OMMP whole conjunctiva and fibroblasts, and also that OMMP fibroblasts have higher ALDH activity than controls. In addition, ALDH is upregulated in the conjunctiva of an established AED mouse model, in which we show the previously unappreciated onset of fibrosis and which demonstrates that this mouse model may be used as a

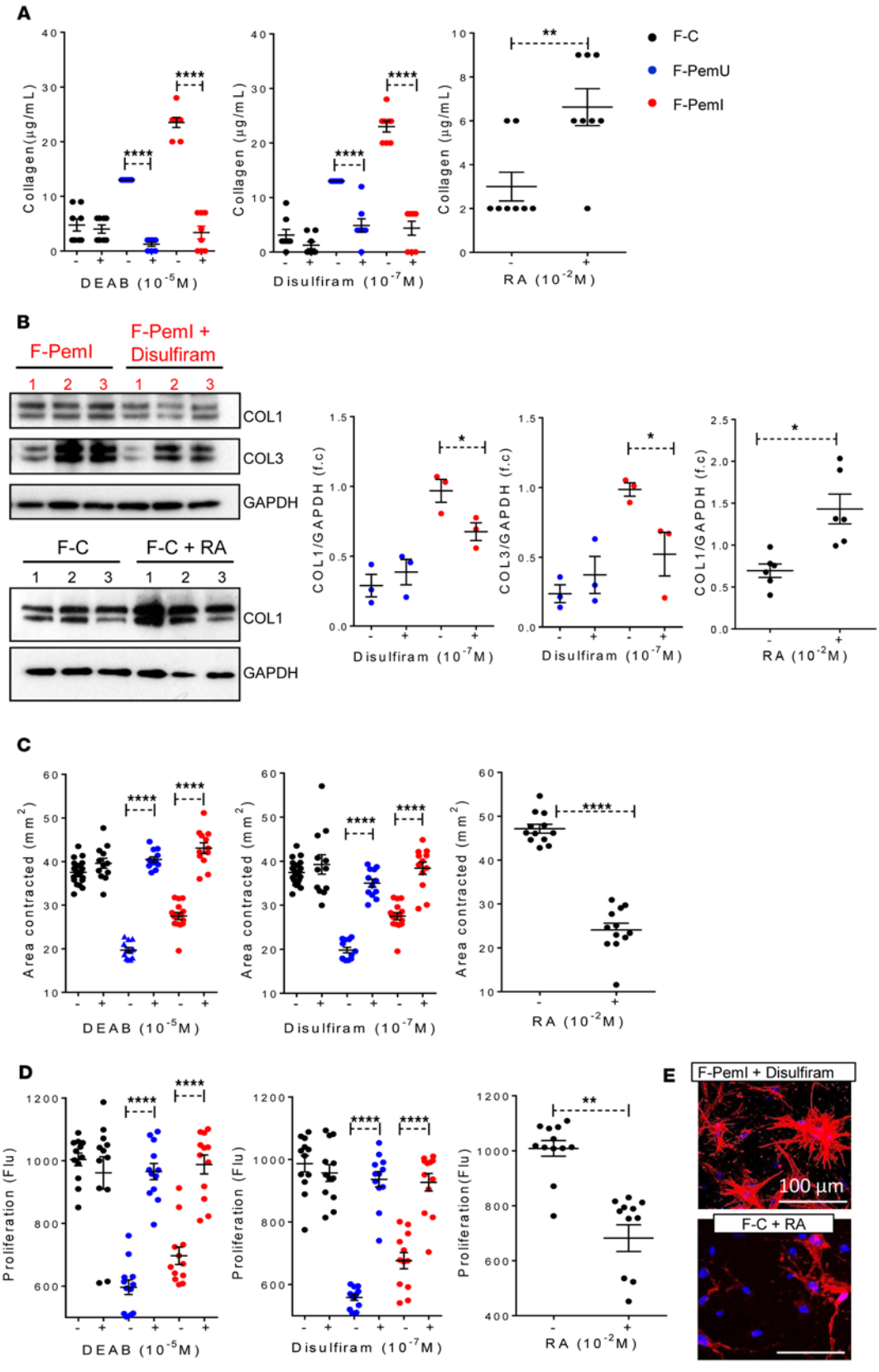

Figure 5. ALDH inhibition decreases collagen production, increases matrix contraction and proliferation, and normalizes αSMA organization of OMMP fibroblasts in vitro. (**A**) Concentration of collagen from F-C (n = 4), F-PemI (n = 4), and F-PemU (n = 4) treated with ALDH inhibitors DEAB, disulfiram, or vehicle. Collagen type 1 was also measured in F-C fibroblasts treated with the ALDH metabolite, retinoic acid, or vehicle. (**B**) Western blotting for (top panel) COL1 and COL3 basal- and disulfiram-treated levels for F-PemI with densitometry panels for both F-PemI and F-PemU (see Supplementary Figure 4 for F-PemU gels). Lower panel shows COL1 basal levels for F-C (n = 3) and ATRA treated F-C (n = 3). (**C**) Area contracted at 72 hours by F-C (n = 4), F-PemI (n = 4), or F-PemU (n = 4) fibroblasts within a free-floating collagen matrix treated with DEAB or disulfiram compared with vehicle, also shown for F-C fibroblasts treated with retinoic acid. (**D**) Fluorescence readings (counts per second [cps]) from F-C (n = 4), F-PemI (n = 4), or F-PemU (n = 4) treated with DEAB, disulfiram, or vehicle and from F-C fibroblasts treated with retinoic acid. (**E**) Representative images of αSMA staining in F-PemI (n = 4) or F-PemU (n = 4) fibroblasts treated with either DEAB (not shown) or disulfiram within tethered collagen matrices. The top panel shows ALDH inhibition increased αSMA organization (compare with normal F-C controls in Figure 4E). Retinoic acid treatment of F-C (n = 4) fibroblasts in a tethered collagen matrix resulted in decreased αSMA organization (bottom panel), similar to that seen in OMMP fibroblasts (as shown in Figure 4E with F-PemI or F-PemU). Each assay was carried out with 4 separate patient fibroblast cultures and at least 3 technical repeats. Error bars represent ±SEM. *P < 0.05, **P < 0.005, ****P < 0.00005 as calculated using one-way ANOVA with Bonferroni correction.

Table 2. CONTROLS (n = 17) (age- and sex-matched with healthy conjunctiva having surgery for cataract of Fuch's corneal dystrophy)

ID	Age	Sex	Race	ID	Age	Sex	Race
C01	87	F	W	C10	85	M	W
C02	77	F	W	C11	86	F	W
C03	64	F	W	C12	77	M	W
C04	54	F	W	C13	76	F	W
C05	93	F	W	C14	55	F	W
C06	86	M	W	C15	84	M	W
C07	74	M	W	C16	81	F	W
C08	78	M	W	C17	68	F	W
C09	86	M	W				

Control patients had healthy conjunctiva. Exclusion criteria for controls are summarised in the first section of online methods. The controls did not have biopsies taken for DIF and had no scarring. W, ethnic white.

surrogate for the study of the mechanisms of inflammation-related conjunctival fibrosis in humans. Using this mouse model, topical application of the ALDH inhibitor disulfiram was shown to decrease conjunctival fibrosis in vivo. Both OMMP fibroblasts and fibroblasts from the inflamed mouse conjunctiva maintain a range of profibrotic characteristics in vitro. Application of ALDH inhibitors in vitro, to both OMMP fibroblasts and fibroblasts from the inflamed mouse conjunctiva, restored their functionality to that of normal controls. The effect of ALDH inhibition on human in vitro OMMP fibroblasts is dose dependent. Conversely, applying RA, a metabolite of ALDH, to human control fibroblasts in vitro induced a diseased phenotype. This evidence suggests that the ALDH1 family has a central role in conjunctival scarring in both OMMP in humans and in immune-mediated conjunctival inflammation and scarring in the mouse; it also suggests that ALDH inhibition is a potential antifibrotic therapy in this setting.

Our findings for cell-associated collagen production, demonstrated by both ELISA and Western blotting, were the same for F-PemI and F-C fibroblasts. However, there was a difference for basal and disulfiram-treated cell-associated collagen levels in F-PemU compared with F-C fibroblasts. When basal levels were measured by Western blotting, there was a trend for increased COL1 levels compared with F-C fibroblasts (Figure 4B), but the significant difference shown by ELISA (Figure 4A) was not apparent. Disulfiram treatment significantly reduced collagen levels by ELISA (Figure 5A) but not when these were measured by Western blotting (Figure 5B). We suggest that these differences are the result of lower-detectable COL1 expression in F-PemU compared with F-PemI, as measured by Western blotting, compared with ELISA because of the potential for the ELISA — which utilized a polyclonal COL1 antibody having cross-reactivity with other COL species — to detect more collagen than the Western blotting, given that COLs I, III, IV, VI, and VII are all found in OMMP whole conjunctiva (31). It is also important to be aware that differences in the levels of clinical inflammation in the human OMMP conjunctiva are points in a continuum of inflammation. The classification of clinically inflamed versus clinically uninflamed utilizes a necessary clincal criterion such that moving the point on the scale, separating clinically uninflamed from inflamed, might affect the differences that we have identified between fibroblasts from uninflamed and inflamed conjunctiva. However, the lack of an inhibitory effect of disulfiram on collagen production shown by the Western blots for F-PemU may mean that fibroblasts that are in a less inflammatory milieu (defined as uninflamed) in whole OMMP tissue could be less susceptible to antifibrotic therapy with ALDH inhibitors.

Our previous study on the phenotype of OMMP fibroblasts showed increased proliferation, no difference in collagen contraction, and increased COLI production compared with control fibroblasts (32), whereas in the current study, although COLI was increased, there was significantly less contraction and reduced proliferation compared with controls. Preliminary experiments for the current studies showed that F-C fibroblasts showed significantly increased contraction and proliferation only for the first outgrowth of fibroblasts from a biopsy (the primary explant) compared with later outgrowths (33). Subsequently, only the primary explant was used for all F-C and F-Pem studies, whereas for the 2011 paper, a mixture of outgrowths from primary and secondary explants were used. We hypothesize that the relative reduction shown for contraction and proliferation of OMMP fibroblasts compared with controls in the current study was due to the increased activity of these parameters in the controls rather than due to a difference in the

OMMP fibroblast phenotype for which increased collagen secretion, arguably the most important characteristic of profibrotic cells, was demonstrated in both studies.

The ALDH superfamily, especially the ALDH1 family and its metabolite RA, has been shown to be important in immunity, inflammation, and scarring, for which the evidence is given below. The 18 enzymes in the ALDH superfamily irreversibly catalyze endogenously and exogenously produced aldehydes to carboxylic acids. ALDH1A3 is one of the ALDH1 subfamilies of ALDHs, which includes ALDH1A1 and ALDH1A2 — for which retinal is the preferred substrate — and which oxidize retinal to RA. This subfamily is irreversibly inhibited by disulfiram. Whereas the ALDH1 family is intimately involved with Vitamin A metabolism, ALDH2 is the key enzyme in alcohol metabolism (29). All-*trans*-RA (ATRA) and 9-*cis*-RA are the metabolically active derivatives of Vitamin A that regulate diverse processes including cellular differentiation, apoptosis, embryonic development, reproduction, and vision in addition to their role in immunity, where they have effects on both the innate and adaptive immune systems (34). RA deficiency is generally associated with a defective immune response, particularly to infection (34). However, several animal studies have shown that RA-driven signals may upregulate the inflammatory response; this reflects human data associating RA therapy with the development of inflammatory bowel disease and pointing to Vitamin A metabolic pathways as potential instigators of chronic inflammation (35). In the gut, RA produced by DCs plays a central role in mucosal immunity, influencing TGFβ-dependent Treg differentiation (36).

RA functions in several ways. ATRA regulates the expression of several hundred genes through binding nuclear RA receptors (RARs including the subfamily retinoic receptor X [RXRs] and activated gene transcription by binding to retinoic acid receptor element [RAREs] in target genes). In addition, ATRA regulates noncoding RNAs. Furthermore, ATRA exerts regulatory effects through nongenomic pathways, largely by modulating protein kinase C (PKC) activity, although other mechanisms have been identified. Lastly, RA may exert modulatory effects through retinoylation of proteins including protein kinase A (37). 9-*cis*-RA, like ATRA, modulates gene expression via RARs (38). The paracrine nature of ALDH/RA activity, how RA itself may also positively upregulate ALDH expression (39), and the close proximity in which DCs and fibroblasts reside in conjunctival stroma (40) provide evidence that suggests DCs and OMMP fibroblasts may maintain ALDH/RA cellular cross-talk between them, ultimately perpetuating OMMP fibroblast dysfunction and fibrosis. We describe an example of this in our companion paper (28)

However, the effects of retinoids may be both profibrotic and antifibrotic depending on the system and model used. These conflicting effects need to be understood when interpreting studies and establishing in vitro models. These complexities have been elegantly described with reference to renal fibrosis (41), which — with hepatic fibrosis (42, 43) — most closely equate to our findings in the OMMP conjunctiva. Rankin et al. give several examples from publications studying lung, liver, and skin in which RA may be either antifibrotic or profibrotic, demonstrating that selectivity of retinoids, cell type-specificity, and choice of profibrotic marker, as well as dose- and condition-dependent factors, may all be important in explaining these seemingly opposing effects (41).

ALDH/RA and TGFβ pathways, depending on the model system, may be either synergistic — as in the induction of Tregs — or antagonistic, resulting in suppression of TGFβ (44). In liver fibrosis, RA directly exacerbates hepatic stellate cell (HSC) function by enhancing plasminogen activator (PA) levels and thereby inducing proteolytic activation of latent TGFβ, resulting in enhanced collagen production (43). In a mouse model of hepatic fibrosis, ALDH3 has also been shown to enhance HSC activation, collagen production, and TGFβ gene expression, promoting liver fibrosis (42). These findings are consistent with our observations in OMMP, and similar mechanisms may be relevant to the mechanism of ALDH/RA and TGFβ interaction in OMMP and resulting fibrosis.

Our hypothesis is that ALDH/RA autoregulation in OMMP fibroblasts may be a rate-limiting step in fibrosis in the two models we have described, independent of an effect on COL gene expression. This might be mediated by similar mechanisms to those described in the studies on liver fibrosis (42, 43), through the induction of the TGF gene, and/or through activation of latent TGFβ by increased PA levels. Active TGFβ then drives both fibroblast activation and ECM production in concert with the numerous other cytokines and growth factors that affect fibroblast activity (45).

The studies described here identify ALDH/RA autoregulation in OMMP fibroblasts as a mechanism underlying progressive conjunctival scarring in this disease. Although this has been recognized in clinical studies, the pathogenesis has been unknown. ALDH/RA autoregulation has been identified as important in adipogenesis in both in vitro and in vivo mouse studies (46). The companion paper by Saban and colleagues

(28), using the AED model described by them in 2012, also provides evidence that DCs mediate induction of pathogenic fibroblast behavior through ALDH/RA paracrine signaling soon after the induction of inflammation. Depletion of the conjunctival DCs, using diphtheria toxin in CD11c DTR GFP mice, or impairing DC-derived ALDH production prevents the development of scar tissue in this model without reducing inflammation. In addition, the profibrotic effect of the RA receptor agonist bexarotene, in this model, identifies the importance of RA in this process. These findings raise the possibility that, in human OMMP, a similar paracrine effect of DCs early in inflammation may result in an abnormal phenotype in fibroblasts, which then develop the capacity to autoregulate, as demonstrated here, and perpetuate the scarring process. The DC/fibroblast interactions shown in the mouse model deserve evaluation in human tissue and may be relevant to the mechanism of ALDH/RA-induced fibrosis in liver and kidney summarized above.

The pathogenesis of inflammation and scarring in OMMP is incompletely understood (3, 23, 47), and our findings implicating the role of pathogenic fibroblast autoregulation, mediated by ALDH/RA, in this process are new. We have shown both that ALDH overexpression can be identified in the conjunctiva and that we can screen for the effects of ALDH inhibition using in vitro–cultured fibroblast assays from phenotyped patients. Other mucosal scarring diseases are potential targets for further study using these techniques. Conjunctival diseases that may share the fibrotic mechanism that we have demonstrated for OMMP are SJS, AKC, and trachoma. Our new finding that the OVA-induced mouse model of severe conjunctival inflammation developed for AED studies (26, 27) can also be used to study inflammation-induced conjunctival fibrosis should provide a valuable tool for further investigation of the mechanisms underlying conjunctival fibrosis. The studies in the companion paper (28) provide evidence for a paracrine effect of DCs on fibroblasts at the initiation of inflammation, and that is also mediated by ALDH/RA.

Collectively, there is evidence — including that from our data — that ALDH has critical roles in inflammation and conjunctival fibrosis and is produced by DCs and fibroblasts. This makes ALDH inhibition, particularly if it can be achieved by local application to affected tissues, an attractive therapeutic target. One of the ALDH inhibitors used in these studies, disulfiram, is already licensed for the treatment of alcohol abuse. The evidence presented suggests that the repurposing of disulfiram, for the topical treatment of conjunctival scarring in OMMP, may result in an effective topical antifibrotic therapy and provides justification for a randomized controlled trial of disulfiram therapy for scarring in OMMP.

Methods

Patient and control subject consent and selection

All biopsies were taken from the bulbar conjunctiva. Biopsies were placed in Leibovitz's L-15 medium (Invitrogen), 10% (v/v) formalin (Sigma-Aldrich) or RNAlater (Qiagen), for explant culture, paraffin-embedding, or RNA extraction. OMMP biopsies were obtained from patients having a diagnosis of MMP confirmed by DIF microscopy, which is required for the gold standard diagnosis of MMP (48). Three phenotypes of patients were included: OMMP patients with conjunctival inflammation (PemI), OMMP patients with an uninflamed conjunctiva after systemic immunosuppression (PemU), and age- and sex-matched control patients with healthy conjunctiva (C) undergoing surgery for cataract or Fuchs' corneal dystrophy. Exclusion criteria for controls included use of any topical medication apart from artificial tears, active secondary malignancy, HIV infection, pregnancy, or breastfeeding. Conjunctival inflammation was assessed from a photographic scale used by the Moorfields Eye Hospital authors (unpublished) and was ≥ 5 (more than minimal) for inflamed compared with uninflamed eyes on a scale ranging from 1–4 for each of the 4 bulbar conjunctival quadrants (maximum score 16). The degree of scarring in the OMMP conjunctiva was measured using the Tauber scoring system (49) in which minimal subconjunctival scarring is scored as stage I, progressing through increasing degrees of lower conjunctival fornix reduction (stage IIa–d) and horizontal involvement by symblepharon (stage IIIa–d [n]), where [n] is the number of symblephara, and finally progressing to a frozen globe (stage IV).

Gene expression microarray

Conjunctival biopsies were immediately put into 500 μl of RNAlater, stored at 4˚C overnight and then frozen at –80˚C until RNA extraction. Tissue samples (C, n = 5; PemI, n = 5; and PemU, n = 5) were homogenized using a Wheaton glass dounce (Fisher Scientific) and then further homogenized with a 19G needle (Fisher Scientific). RNA was isolated from the homogenate using a Qiagen RNeasy kit (Qiagen)

as per the manufacturer's instructions. The gene expression array was carried out at Illumina using the HumanHT-12 v4 BeadChip. Analysis of the data was performed using the method of Burton et al. (50). The microarray data has been deposited in the NCBI Gene Expression Omnibus accessible as GEO series accession number GSE77361. Other than statistical significance, two considerations governed the way in which the microarray data were analyzed. The first related to our hypothesis that an in vitro fibroblast model, using primary conjunctival fibroblasts, could be used to understand more complex in vivo scarring processes. For this reason, we chose to focus only on genes that were differentially expressed in both diseased whole tissue and in diseased fibroblast cultures. The second consideration related to the fact that conjunctival scarring continues to progress in clinically uninflamed conjunctiva (5, 6). This requires therapeutic targets to address the fibrotic process in both clinically inflamed and clinically uninflamed conjunctiva. With these considerations in mind, only those gene transcripts that were differentially expressed (at least 1.5-fold difference, $P < 0.05$) in both PemI and PemU whole conjunctiva, and in F-PemI and F-PemU conjunctival fibroblasts, were selected as potential targets. Only 10 genes met these criteria: *KCNK6*, *CCNF*, *ECGF1*, *BOLA2*, *LGMN*, *HIST1H2BK*, *GFPT1*, *SEC13*, *CD24*, and *ALDH1A3*. At the time of this experiment, the F-C ($n = 2$), F-PemI ($n = 2$), and F-PemU ($n = 2$) fibroblast cultures were available so that qPCR experiments on 4 further donor cultures of each cell type were carried out to confirm the microarray findings.

Histology

Human conjunctival biopsies C ($n = 3$), PemI ($n = 3$), and PemU ($n = 3$) were fixed in 10% (v/v) formalin, processed by the standard methods and embedded in paraffin. Sections (5 μm) were stained for ALDH1A3 using the following IHC protocol. Slides were deparaffinised and pretreated with heat-induced epitope retrieval (HIER) solution and Tris-EDTA Buffer at a pH of 9 for 20 minutes followed by washing in running tap water for 10 minutes. Endogenous peroxidase was quenched by incubating sections in 3% (v/v) H_2O_2 in distilled water. After blocking with Protein Block, Serum-Free for 45 minutes (Dako), the slides were then stained with a rabbit polyclonal antibody to ALDH1A3 (ab12985, Abcam) or rabbit IgG (ab27472, Abcam) 1 μg/ml at 4°C overnight. Antibody binding was visualized using anti–rabbit HRP–labeled IgG (P044801-2, Dako) followed by AEC Substrate System (Vector Laboratories), and the sections were counterstained with Mayer's hematoxylin. Images of the conjunctiva were taken using a Zeiss Axiophot microscope, followed by image analysis using Trio version 1.0.2 software from Caliper Life Sciences.

Whole eyes were obtained from mice ($n = 5$), stored in 10% (v/v) formalin, processed by the standard methods, and embedded in paraffin. Sections (5 μm) were processed and stained with Martius Scarlet Blue stain (MSB) and H&E in the Pathology Core Laboratories (UCL Institute of Ophthalmology). Images were taken of the bulbar conjunctiva using the Motic BA400 light microscope and Moticam 2300 camera.

Conjunctiva excised from whole eyes obtained from mice were fixed in 4% (v/v) paraformaldehyde (PFA) for 1.5 hours and washed 3 times for 5 minutes. The samples were then blocked with 5% (v/v) goat serum (Sigma-Aldrich) in PBS for 30 minutes and subsequently stained with rabbit anti–mouse ALDH1 (ab23375, Abcam), primary antibody in 5% (v/v) goat serum (Invitrogen) for 48 hours at 4°C in the dark. Samples were washed 3 times with PBS, and antibody binding was visualized with goat anti–rabbit AlexaFlour 594 (A-11037, Invitrogen) secondary antibody in 5% (v/v) goat serum in PBS, which was incubated with the samples for 1 hour at room temperature. Samples were washed 5 times with PBS and mounted onto glass coverslips with mounting medium containing DAPI (Vector Laboratories), and images were obtained from a Leica SP8 confocal (Leica Microsystems).

qPCR

Human TaqMan primers for *ALDH1A3* (Hs00167476_m1) and Human *HRPT1* (Hs02800695_m1) genes were purchased from Applied Biosystems. HRPT1 was used to normalize gene expression, as the expression of this gene was stable across the experimental groups. The cDNA was obtained using an Eppendorf Mastercycler, and the qPCR was carried out using the Taqman (Applied Biosystems) on F-C ($n = 4$), F-PemI ($n = 4$), and F-PemU ($n = 4$). To ensure the purity of the cDNA, enzymatic digestion of genomic DNA (gDNA) was incorporated in the isolation of template RNA and in the Qiagen Quantitect reverse transcription kit. The Quantitect reverse transcription step was carried out as per the manufacturer's instructions using 200 ng of RNA per reaction. Each qPCR experiment was run as per the manufacturer's

instructions. The expression level of gene transcripts was standardized relative to that of *HPRT1* in the same reaction using the ΔΔCT method. qPCR was also carried out for COL1A1, COL3A1, and ACTA2 on F-C (n = 3), F-PemU (n = 3), and F-PemI (n = 3) using the Quantifast SYBR Green PCR kit (Qiagen) in a Rotorgene 6000 (Qiagen). TATA binding protein was used as the housekeeping gene (primers: forward 5′- AGTGACCCAGCATCACTGTTT-3′ and reverse 5′-GGCAAACCAGAAACCCTTGC-3′). For the human collagen genes, the following primers were used. COL1A2: forward 5′-TGCTTGCAGTAACCTTATGCCTA-3′ and reverse 5′-CAGCAAAGTTCCCACCGAGA-3′; COL1A1: forward 5′-CCCCTGGAAAGAATGGAGAT-3′ and reverse 5′-AATCCTCGAGCACCCTGA-3′; and COL3A1: forward 5′-TTCTGGAGGATGGTTGCACG-3′ and reverse 5′-GGTAGTCTCACAGCCTTGCG-3′. For the mouse collagen genes, the following primers were used. Col1a2: forward 5′-TAGCCAACCGTGCTTCTC-3′ and reverse 5′-TCTTGCCCCATTCATTTGTC-3′; Col1a1: forward 5′-TGGAAGAGCGGACAGTAC-3′ and reverse 5′-GCGCAGGAAGGTCAGCTG-3′; 18S: forward 5′-TTGACGGAAGGGCACCACCAG-3′ and reverse 5′-GCACCACCACCCACGGAATCG-3′; and Col3a1: forward 5′-CCCACAGCCTTCTACACCTG-3′ and reverse 5′-CCAGGGTCACCATTTCTCCC-3′.

Flow cytometry

Fibroblasts C (n = 3), F-PemI (n = 3), and F-PemU (n = 3) were seeded at 5×10^4 cells/ml in 6-well plates overnight in 37°C with 5% (v/v) CO_2 in air. The cells were trypsinized, centrifuged, and resuspended in ALDEFLOUR buffer (Stemcell Technologies). The samples were then subjected to the ALDEFLOUR assay (Stemcell Technologies) according to the manufacturer's instructions. Samples were analyzed by flow cytometry on a FACScan (BD Biosciences).

SDS-PAGE and Western blotting analysis

Total cell lysates from F-C (n = 3), F-PemU (n = 3), and F-PemI (n = 3) were prepared using ice-cold RIPA extraction buffer. Extraction buffers were supplemented with protease (complete mini; Roche Diagnostics) and phosphatase inhibitors (phosphatase inhibitor cocktails 2 and 3; Sigma-Aldrich). Protein concentration was assessed using the BCA assay (Pierce; Fisher Scientific). Total cell lysates were subjected to Western blot analysis for Collagen Type I (ab758, EMD Millipore), Collagen Type III (ab7778, Abcam), and ACTA2 (A2547, Sigma-Aldrich) expression. The housekeeping gene GAPDH was used as a loading control (ab8245, Abcam). Full uncut gels are shown in Supplemental Figure 4.

Primary conjunctival fibroblast explant cultures

The biopsy was placed under a coverslip and air dried at 37°C with 5% (v/v) CO_2 in air for 30–35 minutes. Conjunctival fibroblast medium consisting of 10% (v/v) FCS (Invitrogen) and 1× (50 IU/ml) antibiotic-antimycotic (Invitrogen) in DMEM plus Glutamax (Invitrogen) was then added to the biopsy sample. When cells that grew out the biopsy reached at least 60% confluency (2–4 weeks after coverslip application), they were trypsinized and passaged. Subsequently, cells were passaged (1 in 3) once per week at 60% confluency. Fibroblasts were primarily characterized by their spindle-shaped morphology and were passaged up to passage 7. For experiments, cells that were between passages 4–7 were utilized.

Fibroblast assays

For each assay, F-C (n = 4), F-PemI (n = 4), and F-PemU (n-4) were used.

Collagen production ELISA. Fibroblasts (3×10^4 cells/well) were seeded in 24-well plates for 24 hours. The cells were lysed using 0.05 M acetic acid (Sigma-Aldrich), and then a 2-step digestion process using pepsin (Sigma-Aldrich) and pancreatic elastase (Sigma-Aldrich) was carried out to solubilize intracellular collagen. Collagen was solubilized and measured using a Collagen type 1 ELISA (MD Bioproducts) according to the manufacturer's protocol.

Collagen production Sircol. Media was collected from the fibrobast cultures used to evaluate intracellular collagen production and assayed for the presence of secreted collagen. Collagen released into the media by the fibroblasts was analyzed using the Sircol assay. An additional step of solubilizing the collagen with pepsin (Sigma-Aldrich), 0.1 mg/ml, 0.5 M acetic acid was carried out to solubilize the collagen. The solubilization and quantification of the collagen was carried out according to the manufacturer's protocol.

Matrix contraction assays. Fibroblasts (125 μl, 1.6×10^6 cells/ml) and 10× MEM (125 μl; Invitrogen) were added to 1 ml of collagen type 1 solution (2 mg/ml; First Link) dissolved in 0.6% (v/v) acetic acid

that was previously neutralized with 5 M NaOH (Sigma-Aldrich). The collagen/fibroblast mixture (60 μl) was pipetted into individual wells of a 96-well plate and left to set at 37°C for 30 minutes in 5% (v/v) CO_2 in air. Conjunctival fibroblast medium was added to each of the gels, and the gels were released from the edges of the wells. The gels were incubated at 37°C in a humidified atmosphere of 5% (v/v) CO_2 in air. Images were taken of the gels on day 1, 2, and 3 using an ELPH 340 Canon camera, and the gel areas were measured using NIH Image J.

Proliferation assay. Fibroblast proliferation was analyzed using the CyQuant proliferation assay (Invitrogen). Fibroblasts (100 μl, 5×10^4 cells/ml) were seeded in a 96-well plate, and then the CyQuant proliferation assay was carried out as per the manufacturer's protocol.

αSMA expression. Expression of αSMA was assessed by confocal microscopy of tethered collagen type 1 gels populated with fibroblasts. The gels were formed in the same manner as the free-floating gels in the contraction assay. However, after the gels were set and the conjunctival fibroblast medium was added, the gels were not released from the edges of the well. After 24 hours, the gels were stained with αSMA antibody that was directly conjugated with Cy3 (Sigma-Aldrich) using the staining protocol recommended by the manufacturer. Confocal microscopy was carried out using the Zeiss LSM 710 followed by image analysis with Zeiss (Zen) software.

Preparation of ALDH inhibitors and ATRA

For in vitro experiments, DEAB (Sigma-Aldrich), disulfiram (Tocris Biosciences), and ATRA (Sigma-Aldrich) were all initially dissolved in 100% DMSO forming 100 mM stock solutions. Inhibitors were subsequently diluted in PBS (Invitrogen) such that the final concentration of DMSO was 0.01% (v/v). Vehicle was 0.01% DMSO.

For in vivo experiments, disulfiram (300 μM) was dissolved in distilled water. DEAB was dissolved to 600 mM in 100% ethanol and then diluted into a working concentration of 300 μM DEAB in PBS containing 0.01% (v/v) ethanol. The vehicle for DEAB was PBS containing 0.01% (v/v) ethanol, and for disulfiram, distilled water was the vehicle control.

Animal model

Immune-mediated conjunctivitis was induced in C57/BL6 mice (Charles River Laboratories) by i.p. injection of 200 μl of immunization mix containing: OVA (10 μg; Sigma-Aldrich), aluminium hydroxide (4 mg; Thermo Scientific), and pertussis toxin (300 ng; Sigma-Aldrich). After 2 weeks, mice received topical OVA challenge once a day for 7 days. Both eyes of each mouse were challenged and scored in the same manner. For the scoring, a cumulative score was taken from the scores of eyelid swelling (out of 3) and tearing (out of 3). As clinical manifestations were uniformly present in all mice, 5 mice were used per experimental group.

Statistics

For each in vitro fibroblast assay, more than triplicate data points were collected from at least 3 separate fibroblast cultures from separate donor conjunctival tissue, and the experiments were repeated at least twice. Where whole tissue samples were utilized, for example in the microarray, at least 5 independent donor samples were used. For the in vivo experiments, there were 5 mice per experimental condition, as disease was consistently exhibited across all mice. Analysis for ±SEM and statistical significance for all experiments was carried out by 1-way ANOVA followed by Bonferonni correction. $P < 0.05$ was considered significant.

Study approval

Conjunctival biopsies were taken from patients with consent and ethical approval from the local ethics committee (Hertfordshire REC reference 10/H0311/40, Protocol SAWV1005).

Author contributions

SDA, DJA, JTD, VLC, and JKD contributed to this manuscript by designing research studies, conducting experiments, acquiring data, analyzing data, and writing the manuscript. JTN, SR, and MP conducted experiments, acquired data, analyzed data, and contributed to the writing of the manuscript. JKD recruited patients and provided tissue, as did VPS, who contributed to writing the manuscript. DRS and VLC provided reagents and contributed to writing the manuscript.

Acknowledgments

The authors would like to thank Elaina Reid (research nurse, Moorfields Eye Hospital NHS Foundation Trust) for assistance with the patient related aspects and Alan Holmes (Centre for Rheumatology and Connective Tissue Diseases, University College London, Royal Free Campus) for assistance with interpretation of the gene expression microarray. We thank the following organizations and donors for funding these studies: the NIHR Biomedical Research Centre for Ophthalmology Major Award to support translational research initiatives (BMRC 045), a Fight for Sight PhD studentship (1818), Anonymous Donors through MEH Special Trustees (ST1111D, ST1304E), and UCL Business Proof of Concept Funding (PoC-14-010).

Address correspondence to: John K. Dart, 162 City Rd, London, EC1V 2PD, United Kingdom. Phone: 44.20.7566.2320; E-mail: j.dart@ucl.ac.uk.

1. Rockey DC, Bell PD, Hill JA. Fibrosis--a common pathway to organ injury and failure. *N Engl J Med.* 2015;372(12):1138–1149.
2. Schmidt E, Zillikens D. Pemphigoid diseases. *Lancet*. 2013;381(9863):320–332.
3. Kasperkiewicz M, Zillikens D, Schmidt E. Pemphigoid diseases: pathogenesis, diagnosis, and treatment. *Autoimmunity*. 2012;45(1):55–70.
4. Hardy KM, Perry HO, Pingree GC, Kirby TJ. Benign mucous membrane pemphigoid. *Arch Dermatol*. 1971;104(5):467–475.
5. Saw VP, et al. Immunosuppressive therapy for ocular mucous membrane pemphigoid strategies and outcomes. *Ophthalmology*. 2008;115(2):253–261.e1.
6. Williams GP, Radford C, Nightingale P, Dart JK, Rauz S. Evaluation of early and late presentation of patients with ocular mucous membrane pemphigoid to two major tertiary referral hospitals in the United Kingdom. *Eye (Lond).* 2011;25(9):1207–1218.
7. Radford CF, Rauz S, Williams GP, Saw VP, Dart JK. Incidence, presenting features, and diagnosis of cicatrising conjunctivitis in the United Kingdom. *Eye (Lond).* 2012;26(9):1199–1208.
8. Saw VP, Dart JK. Ocular mucous membrane pemphigoid: diagnosis and management strategies. *Ocul Surf*. 2008;6(3):128–142.
9. Foster CS. Cicatricial pemphigoid. *Trans Am Ophthalmol Soc*. 1986;84:527–663.
10. Sacher C, Hunzelmann N. Cicatricial pemphigoid (mucous membrane pemphigoid): current and emerging therapeutic approaches. *Am J Clin Dermatol*. 2005;6(2):93–103.
11. Chang JH, McCluskey PJ. Ocular cicatricial pemphigoid: manifestations and management. *Curr Allergy Asthma Rep*. 2005;5(4):333–338.
12. Chan LS. Ocular and oral mucous membrane pemphigoid (cicatricial pemphigoid). *Clin Dermatol*. 2012;30(1):34–37.
13. Mondino BJ, Brown SI. Ocular cicatricial pemphigoid. *Ophthalmology*. 1981;88(2):95–100.
14. Sobolewska B, Deuter C, Zierhut M. Current medical treatment of ocular mucous membrane pemphigoid. *Ocul Surf*. 2013;11(4):259–266.
15. Sacks EH, Jakobiec FA, Wieczorek R, Donnenfeld E, Perry H, Knowles DM. Immunophenotypic analysis of the inflammatory infiltrate in ocular cicatricial pemphigoid. Further evidence for a T cell-mediated disease. *Ophthalmology*. 1989;96(2):236–243.
16. Saw VP, Dart RJ, Galatowicz G, Daniels JT, Dart JK, Calder VL. Tumor necrosis factor-alpha in ocular mucous membrane pemphigoid and its effect on conjunctival fibroblasts. *Invest Ophthalmol Vis Sci*. 2009;50(11):5310–5317.
17. Bernauer W, Wright P, Dart JK, Leonard JN, Lightman S. Cytokines in the conjunctiva of acute and chronic mucous membrane pemphigoid: an immunohistochemical analysis. *Graefes Arch Clin Exp Ophthalmol*. 1993;231(10):563–570.
18. Caproni M, et al. Cytokine profile and supposed contribution to scarring in cicatricial pemphigoid. *J Oral Pathol Med*. 2003;32(1):34–40.
19. Saw VP, et al. Conjunctival interleukin-13 expression in mucous membrane pemphigoid and functional effects of interleukin-13 on conjunctival fibroblasts in vitro. *Am J Pathol*. 2009;175(6):2406–2415.
20. Lambiase A, et al. T-helper 17 lymphocytes in ocular cicatricial pemphigoid. *Mol Vis*. 2009;15:1449–1455.
21. Elder MJ, Dart JK, Lightman S. Conjunctival fibrosis in ocular cicatricial pemphigoid--the role of cytokines. *Exp Eye Res*. 1997;65(2):165–176.
22. Razzaque MS, Ahmed BS, Foster CS, Ahmed AR. Effects of IL-4 on conjunctival fibroblasts: possible role in ocular cicatricial pemphigoid. *Invest Ophthalmol Vis Sci*. 2003;44(8):3417–3423.
23. Kourosh AS, Yancey KB. Pathogenesis of mucous membrane pemphigoid. *Dermatol Clin*. 2011;29(3):479–484.
24. Kirzhner M, Jakobiec FA. Ocular cicatricial pemphigoid: a review of clinical features, immunopathology, differential diagnosis, and current management. *Semin Ophthalmol*. 2011;26(4-5):270–277.
25. Saw VP, et al. Profibrotic phenotype of conjunctival fibroblasts from mucous membrane pemphigoid. *Am J Pathol*. 2011;178(1):187–197.
26. Lee HS, Schlereth S, Khandelwal P, Saban DR. Ocular allergy modulation to hi-dose antigen sensitization is a Treg-dependent process. *PLoS One*. 2013;8(9):e75769.
27. Schlereth S, Lee HS, Khandelwal P, Saban DR. Blocking CCR7 at the ocular surface impairs the pathogenic contribution of dendritic cells in allergic conjunctivitis. *Am J Pathol*. 2012;180(6):2351–2360.
28. Ahadome SD, et al. Classical dendritic cells mediate fibrosis directly via the retinoic acid pathway, in severe eye allergy. *JCI Insight*. 2016;1(12):e87012.
29. Koppaka V, et al. Aldehyde dehydrogenase inhibitors: a comprehensive review of the pharmacology, mechanism of action, substrate specificity, and clinical application. *Pharmacol Rev*. 2012;64(3):520–539.
30. Cvek B, Dvorak Z. Targeting of nuclear factor-kappaB and proteasome by dithiocarbamate complexes with metals. *Curr Pharm Des*. 2007;13(30):3155–3167.

31. Dutt JE, Ledoux D, Baer H, Foster CS. Collagen abnormalities in conjunctiva of patients with cicatricial pemphigoid. *Cornea*. 1996;15(6):606–611.
32. Saw VP, et al. Profibrotic phenotype of conjunctival fibroblasts from mucous membrane pemphigoid. *Am J Pathol*. 2011;178(1):187–197.
33. Dale S. *Aldehyde dehydrogenase as a novel potential therapy for conjunctival fibrosis* [dissertation]. London: University College London; 2014.
34. Stephensen CB. Vitamin A, infection, and immune function. *Annu Rev Nutr*. 2001;21:167–192.
35. Hall JA, Grainger JR, Spencer SP, Belkaid Y. The role of retinoic acid in tolerance and immunity. *Immunity*. 2011;35(1):13–22.
36. Manicassamy S, Pulendran B. Retinoic acid-dependent regulation of immune responses by dendritic cells and macrophages. *Semin Immunol*. 2009;21(1):22–27.
37. Blomhoff R, Blomhoff HK. Overview of retinoid metabolism and function. *J Neurobiol*. 2006;66(7):606–630.
38. Xu Q, Kopp JB. Retinoid and families: crosstalk in development, neoplasia, immunity, and tissue repair. *Semin Nephrol*. 2012;32(3):287–294.
39. Stock AT, Bedoui S. Vitamin A notches up CD11b hi DC development. *Eur J Immunol*. 2013;43(6):1441–1444.
40. Saalbach A, et al. Dermal fibroblasts induce maturation of dendritic cells. *J Immunol.* 2007;178(8):4966–4974.
41. Rankin AC, Hendry BM, Corcoran JP, Xu Q. An in vitro model for the pro-fibrotic effects of retinoids: mechanisms of action. *Br J Pharmacol*. 2013;170(6):1177–1189.
42. Yi HS, et al. Alcohol dehydrogenase III exacerbates liver fibrosis by enhancing stellate cell activation and suppressing natural killer cells in mice. *Hepatology*. 2014;60(3):1044–1053.
43. Okuno M, et al. Retinoids in liver fibrosis and cancer. *Front Biosci.* 2002;7:d204–d218.
44. Liang X, Liu Z, Lin Y, Li N, Huang M, Wang Z. A modified symblepharon ring for sutureless amniotic membrane patch to treat acute ocular surface burns. *J Burn Care Res.* 2012;33(2):e32–e38.
45. Wick G, Backovic A, Rabensteiner E, Plank N, Schwentner C, Sgonc R. The immunology of fibrosis: innate and adaptive responses. *Trends Immunol*. 2010;31(3):110–119.
46. Reichert B, et al. Concerted action of aldehyde dehydrogenases influences depot-specific fat formation. *Mol Endocrinol.* 2011;25(5):799–809.
47. Dart JKG, Saw VPJ. Immune Modulation in Ocular Mucous Membrane Pemphigoid. In Pleyer U, Alió J, Barisani-Asenbauer T, Le Hoang P, Rao NA, eds. *Immune Modulation and Anti-Inflammatory Therapy in Ocular Disorders.* Heidelberg, Germany: Springer-Verlag; 2014:19-39.
48. Chan LS, et al. The first international consensus on mucous membrane pemphigoid: definition, diagnostic criteria, pathogenic factors, medical treatment, and prognostic indicators. *Arch Dermatol*. 2002;138(3):370–379.
49. Tauber J, Jabbur N, Foster CS. Improved detection of disease progression in ocular cicatricial pemphigoid. *Cornea*. 1992;11(5):446–451.
50. Burton MJ, et al. Conjunctival transcriptome in scarring trachoma. *Infect Immun*. 2011;79(1):499–511.